Received: 21 September 2018 | Revised: 22 February 2019 | Accepted: 26 February 2019

DOI: 10.1002/hbm.24565

WILEY

RESEARCH ARTICLE

Gesturing tool use and tool transport actions modulates inferior parietal functional connectivity with the dorsal and ventral object processing pathways

Frank E. Garcea[1,2] | Laurel J. Buxbaum[1,3]

[1]Moss Rehabilitation Research Institute, Albert Einstein Healthcare Network, Elkins Park, Pennsylvania

[2]Cognitive Neuroscience, University of Pennsylvania, Philadelphia, Pennsylvania

[3]Department of Rehabilitation Medicine, Thomas Jefferson University, Philadelphia, Pennsylvania

Correspondence
Frank E. Garcea, Moss Rehabilitation Research Institute, Elkins Park, PA 19027.
Email: garceafr@einstein.edu

Funding information
National Institutes of Health, Grant/Award Number: R01 NS099061 and 5T32HD071844-05

Abstract

Interacting with manipulable objects (tools) requires the integration of diverse computations supported by anatomically remote regions. Previous functional neuroimaging research has demonstrated the left supramarginal (SMG) exhibits functional connectivity to both ventral and dorsal pathways, supporting the integration of ventrally-mediated tool properties and conceptual knowledge with dorsally-computed volumetric and structural representations of tools. This architecture affords us the opportunity to test whether interactions between the left SMG, ventral visual pathway, and dorsal visual pathway are differentially modulated when participants plan and generate tool-directed gestures emphasizing functional manipulation (tool use gesturing) or structure-based grasping (tool transport gesturing). We found that functional connectivity between the left SMG, ventral temporal cortex (bilateral fusiform gyri), and dorsal visual pathway (left superior parietal lobule/posterior intraparietal sulcus) was maximal for tool transport planning and gesturing, whereas functional connectivity between the left SMG, left ventral anterior temporal lobe, and left frontal operculum was maximal for tool use planning and gesturing. These results demonstrate that functional connectivity to the left SMG is differentially modulated by tool use and tool transport gesturing, suggesting that distinct tool features computed by the two object processing pathways are integrated in the parietal lobe in the service of tool-directed action.

KEYWORDS

dorsal stream, functional connectivity, functional magnetic resonance imaging, left supramarginal gyrus, manipulable object representations, tool processing, tool transport, tool use, ventral stream

1 | INTRODUCTION

Tool-directed grasping and tool use ability forms a core aspect of human cognitive function that is utilized on a moment-to-moment basis. Consider for example the difference between grasping a pair of scissors to pass to a friend and grasping a pair of scissors to cut a piece of paper: In the former, one can grasp the scissors in a number of ways depending on biomechanical comfort and given environmental constraints such as the location of the object with respect to the body, limbs, and hands; in contrast, in order to use scissors to cut paper one must arrange the hand and fingers in a manner that presupposes the retrieval of conceptual/functional knowledge for skilled object manipulation. Understanding how functional interactions among object representations in the ventral and dorsal pathways support tool use has been the focus of recent neurocognitive proposals of action representation in the brain (e.g., see Buxbaum, 2017; Cloutman, 2013; Freud, Plaut, & Behrmann, 2016; Mahon & Caramazza, 2011; Milner, 2017; Orban & Caruana, 2014; van Polanen & Davare, 2015). In this report we use functional connectivity based functional magnetic resonance imaging (fMRI) in a group of neurotypical volunteers to assess whether gesturing to move or transport a tool relies on qualitatively different functional interactions than when gesturing to functionally manipulate or use a tool.

Functional neuroimaging work focusing on tool processing has demonstrated that the retrieval of object manipulation knowledge, or physically generating tool use actions, elicits increased blood

oxygen level-dependent (BOLD) signal in the left supramarginal gyrus (SMG; Boronat et al., 2005; Brandi, Wohlschlager, Sorg, & Hermsdorfer, 2014; Buchwald, Przybylski, & Kroliczak, 2018; Buxbaum, Kyle, Tang, & Detre, 2006; Canessa et al., 2008; Chen, Garcea, Jacobs, & Mahon, 2018; Chen, Garcea, & Mahon, 2016; Gallivan, McLean, Valyear, & Culham, 2013; Hermsdorfer, Terlinden, Muhlau, Goldenberg, & Wohlschlager, 2007; Johnson-Frey, Newman-Norlund, & Grafton, 2005; Kellenbach, Brett, & Patterson, 2003; Rumiati et al., 2004), whereas more superior regions in bilateral anterior and posterior intraparietal sulcus (IPS), and superior parietal-occipital cortex respond maximally when reaching to touch or grasp objects (for review, see Gallivan & Culham, 2015; Konen, Mruczek, Montoya, & Kastner, 2013).

A separate functional neuroimaging literature has focused on the representation of tools in the ventral visual pathway, and has demonstrated that viewing images of tools, relative to common baseline categories (e.g., animals, conspecifics), elicits increased BOLD contrast in bilateral medial fusiform gyri (Chao, Haxby, & Martin, 1999; Devlin, Rushworth, & Matthews, 2005; Garcea & Mahon, 2014; Mahon et al., 2007; Noppeney, Price, Penny, & Friston, 2006), left posterior middle temporal gyrus (Beauchamp, Lee, Haxby, & Martin, 2002; Chao et al., 1999; Kristensen, Garcea, Mahon, & Almeida, 2016; Mahon, Anzellotti, Schwarzbach, Zampini, & Caramazza, 2009; for review, see Lewis, 2006; A. Martin, 2007), and in the left middle occipital gyrus ("dorsal occipital cortex," for example, see Garcea, Chen, Vargas, Narayan, & Mahon, 2018; Garcea, Kristensen, Almeida, & Mahon, 2016; Garcea & Mahon, 2014; for review see Lingnau & Downing, 2015). Other studies have shown that viewing images of typical functional grasps, relative to atypical functional grasps, engages lateral temporooccipital cortex in the vicinity of the left posterior middle temporal gyrus and lateral occipital cortex (e.g., see Valyear & Culham, 2010; see also Buxbaum et al., 2006).

A third parallel literature has focused on the representation of manipulable objects outside of parietal and temporooccipital regions. For example, Anzellotti, Mahon, Schwarzbach, and Caramazza (2011) demonstrated that categorizing images of tools (relative to categorizing images of animals) led to differential BOLD contrast in the left ventral anterior temporal lobe (for neuropsychological evidence, see Brambati et al., 2006). Several repetitive transcranial magnetic stimulation (rTMS) studies have found that stimulation to the left anterior temporal lobe selectively slowed down conceptual/function judgments of tools but had no effect when participants made judgments about tool manipulation (Ishibashi, Lambon Ralph, Saito, & Pobric, 2011; see also Andres, Pelgrims, & Olivier, 2013; Pelgrims, Olivier, & Andres, 2011; Pobric, Jefferies, & Ralph, 2010), indicating that function knowledge of tools is represented in part in the left ventral anterior temporal lobe. Other studies reported the involvement of the left ventral premotor cortex (Chao & Martin, 2000; Grafton, Fadiga, Arbib, & Rizzolatti, 1997; Kroliczak & Frey, 2009), the left inferior frontal gyrus (IFG) bordering pars opercularis (e.g., see Johnson-Frey et al., 2003), and the left insula (Brandi et al., 2014) when participants viewed tool images or were instructed to process the appropriate manner with which to grasp or manipulate objects. Neuropsychological evidence consistent with those fMRI findings suggests that lesions to the left IFG and adjacent structures in the insula impair the ability to select the appropriate manner with which to grasp or use an object (e.g., see Watson & Buxbaum, 2015; see also Goldenberg, Hermsdorfer, Glindemann, Rorden, & Karnath, 2007; Martin et al., 2016).

Collectively, these studies suggest that the processing of manipulable objects engages a broad network of regions involved in conceptual processing of tools and their associated actions, which must be integrated with information extracted online about object structure and volume for the programming of arm and hand movements; furthermore, that information must interface with mechanisms involved in the selection of task-appropriate actions for subsequent object use. A recent neurocognitive model (the "Two Action Systems Plus Account"; 2AS+) advanced by Buxbaum, Binkofski and colleagues (Binkofski & Buxbaum, 2013; Buxbaum, 2017) articulates how tool-related information may be integrated in the service of interacting with and manipulating tools. Based in part on evidence from the macaque brain (Rizzolatti & Matelli, 2003), it has been argued that the dorsal visual pathway can be subdivided into two anatomically and computationally independent (but highly interactive) pathways for action processing. The dorso-dorsal pathway transforms current visual input into a sensory-motor representation in the service of reaching and grasping, supported in part by bilateral IPS, superior parietal-occipital cortex, and dorsal premotor cortex. In contrast, the ventro-dorsal pathway supports the transformation of visual information from environmental input and from stored representations of action appearance into a sensory-motor representation for functional manipulation and tool use, supported in part by the left SMG, left ventral premotor cortex, and left IFG.

While both pathways function independently, it is through the integration of conceptual representations of tools and their associated actions supported in part by the ventral stream with online sensory-motor information extracted in part by the dorso-dorsal stream that "manipulation knowledge" is aggregated in the left SMG, a portion of the ventro-dorsal stream, and transiently buffered. A biasing signal from the left IFG enables selection of task-appropriate actions and subsequent relaying of the selected action to the motor system (see also Cisek & Kalaska, 2010; Schubotz, Wurm, Wittmann, & von Cramon, 2014).

A prediction derived in part from the 2AS+ model, which forms a principal motivation for this study, is that functional connectivity to the left SMG should be modulated by action tasks emphasizing different tool-directed computations. To date, the available evidence suggests only that action versus nonaction tasks differentially modulate the tool use network. For example, Garcea et al. (2018) asked a group of participants to pantomime the use of objects or to perform an *n*-back style picture matching task, and measured the degree to which functional connectivity was differentially driven by task. The items and stimulus presentation parameters were identical across tasks, thus any changes in connectivity were driven by the computations engaged by the task over and above the items used. Garcea and colleagues found that functional connectivity between the left SMG and ventral visual pathway (left medial fusiform gyrus) exhibited strong functional connectivity during the picture matching experiment, whereas functional connectivity between the left SMG, left middle temporal gyrus, left dorsal and ventral premotor cortex was maximal during the tool

pantomiming experiment (see Chen, Garcea, Almeida, & Mahon, 2017; Hutchison & Gallivan, 2018; Kleineberg et al., 2018).

Here we use a similar experimental approach to extend prior observations and to contrast functional connectivity modulated when gesturing tool use actions against functional connectivity modulated when gesturing tool transport actions. We used a sparse event-related design to quantify functional connectivity as a function of planning and gesturing tool use actions separately from tool transport actions, and compared changes in functional connectivity over and above modulations of functional connectivity observed during baseline fixation events. Importantly, the same stimuli and stimulus presentation parameters were maintained across tool use and transport conditions, thus any observed changes in functional connectivity would be driven by computations engaged by the task over and above the stimuli used. Although tool use gestures are more heterogenous and diverse in the range and complexity of movement relative to tool transport gestures, we included tool transport planning and gesturing to serve as an important contrast to demonstrate that changes in functional connectivity for tool use would not be driven by *any* engagement of the hand and fingers to produce an action. In addition, we sought positive evidence that tool transport planning and gesturing may differentially modulate functional connectivity relative to tool use planning and gesturing.

We sought to test four predictions. First, we predicted that generating tool use actions, relative to tool transport actions, should elicit differential BOLD contrast in the left SMG, left middle temporal gyrus, and left IFG. Given low-level motor differences between the gesturing of tool use actions relative to tool transport actions, we focused our BOLD contrast analyses on the planning phase. Second, we predicted that planning and generating tool use gestures should emphasize conceptual processing of tools and their associated actions, which should be reflected in increased functional connectivity between the left SMG, left middle temporal gyrus, and left ventral anterior temporal lobe. Third, we predicted that planning and gesturing tool use emphasizes the selection of task-appropriate actions from competing alternatives, which should elicit increased functional connectivity between the left SMG and left IFG. Finally, we predicted that planning and generating tool transport gestures, by hypothesis, bypasses semantic processing and emphasizes sensory-motor processing of the stimulus, which should be reflected in increased functional connectivity between the left SMG and the dorso-dorsal stream (left posterior IPS/superior parietal cortex).

As a secondary aim, we assessed whether interactions between the left SMG and ventral temporal cortex (bilateral medial fusiform gyri) were differentially modulated by action type. Adjacent voxels in the left and right collateral sulci have been shown to respond to surface texture of objects more than to object form or orientation (e.g., see Cant & Goodale, 2007). What remains poorly understood is whether representations of material properties (e.g., surface texture) are differentially relevant when planning and generating tool use or tool transport gestures; thus we assessed how and whether interactions between the left SMG and bilateral ventral temporal cortex were differentially driven by tool use versus tool transport gesturing.

2 | METHODS

2.1 | Participants

Thirty-four volunteers (16 females; mean age, 22 years; *SD*, 2.6 years) from the University of Pennsylvania participated in the study in exchange for payment. All participants were native English speakers, had normal or corrected-to normal vision, had no history of neurological illness, and were right hand dominant (established with the Edinburgh Handedness Questionnaire; Oldfield, 1971). All participants gave written informed consent in accordance with the Institutional Review Board at the University of Pennsylvania and the Albert Einstein Healthcare Network. One participant's data were removed due to excessive head movement (>2 *SD* of movement in translation and rotation in *XYZ* dimensions); all subsequent analyses were performed over the remaining 33 participants.

2.2 | General experimental procedure

Stimulus presentation was controlled with E-Prime Professional Software 2.0 (Psychology Software Tools, Inc., Sharpsburg, PA). All participants viewed the stimuli binocularly through a mirror attached to the head coil adjusted to allow for foveal viewing of a back-projected monitor (temporal resolution = 60 Hz). Each participant took part in one scanning session which began with a high resolution T1 anatomical scan; 22 of the 33 participants then took part in four runs of an object recognition experiment not germane to the focus of this study (using different stimuli), followed by two runs of the experiment proper. A second cohort of 12 individuals participated in a T1 anatomical scan, followed by eight runs of the experiment proper. We collected eight runs in those individuals to study the neural mechanisms supporting pantomiming of tool use not germane to the focus of this study; we include only the first two runs of data from these 12 additional participants to ensure that all participants contributed equal amounts of data to subsequent BOLD contrast and functional connectivity analyses.

2.3 | Tool viewing, planning, and pantomiming fMRI experiment

2.3.1 | Design

There were 12 cells in the design of the experiment: Task type (three levels; view, plan, pantomime), Action type (two levels; tool use, tool transport), and Conflict type (two levels; high conflict items, low conflict items; see Watson & Buxbaum, 2015). (We collapse across conflict type in the focused analyses reported here, resulting in a design with six cells.) Eight photographs of manipulable objects (scissors, cork screw, key, screwdriver, axe, bottle opener, butcher knife, and fork) were presented in a sparse event-related design; there was one exemplar of each item, and each item was presented once per run (for original items, see Watson & Buxbaum, 2015;[1] see Figure 1 for a schematic of the trial

[1]The eight tool items are part of a larger battery of 40 objects used to test pantomime ability in limb apraxic patients; items were independently equated for number of affordances, name agreement, and familiarity; six of the eight items were equated for average number of moveable parts. For details see Watson & Buxbaum, 2015.

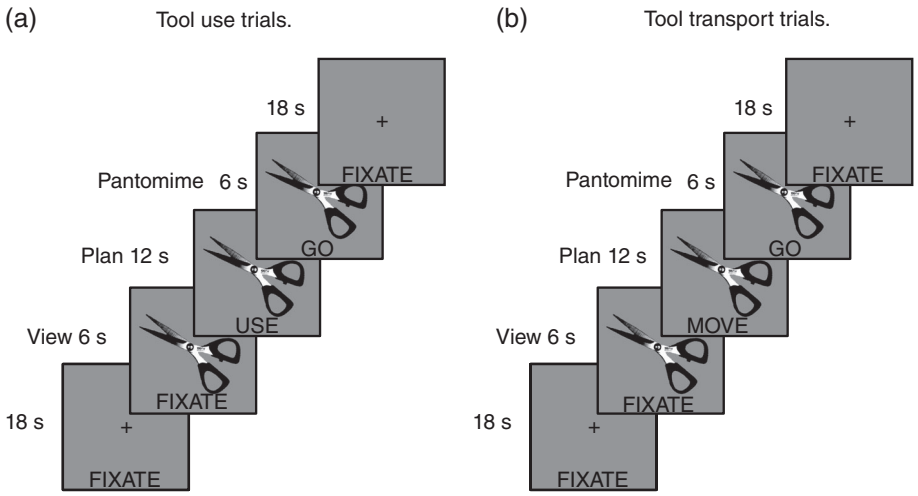

FIGURE 1 Schematic of trial structure in the tool viewing, planning, and pantomiming fMRI experiment. (a) Tool use pantomiming epochs began with 18 s of fixation, followed by the visual presentation of a manipulable object. For 6 s the image was presented with the word "FIXATE" presented underneath it and participants were directed to fixate on and pay attention to the object. Then, an action cue word replaced the fixation instruction and participants were directed to think about and plan interacting with the presented object to use it. After 12 s the action cue was replaced with the word "GO" and participants were instructed to repetitively generate a tool use action (~1 movement per second) for the duration of the go signal. After 6 s the tool image and go cue were replaced with a fixation event and participants were instructed to relax and remain still until the next trial. (b) Tool transport pantomiming epochs were identical to tool use pantomiming events in timing and stimulus presentation parameters except that participants were instructed to think about and plan interacting with the presented object to move it (e.g., displace it 6 in.). Participants generated repetitive tool transport actions when the go cue was presented (~1 movement per second), and were instructed to relax and remain still during the fixation events interposed between epochs

structure). The assignment of items to action type was counterbalanced within- and across-runs in an ABAB format. At the item level, half of the tools assigned to tool use events on odd runs were assigned to tool transport events on even runs (and vice versa for the other half of tools), such that after two runs every item was presented in every cell of the design. Tool use and tool transport trials were presented randomly within a run. Pictorial and word stimuli were centrally presented to allow for foveal viewing and to minimize eye movements.

2.3.2 | Procedure

During each 24-second trial, a picture of a tool was presented centrally for the duration of the event; the first 6 s of each trial began with the image and with the word "FIXATE" presented below it. During these "viewing" events participants were instructed to pay attention to the presented image. After 6 s the "FIXATE" cue was replaced with the word "MOVE" or "USE," which remained for 12 s. The word served as a cue for participants to begin planning and imagining interacting with the object in order to move it (i.e., interacting with the object to pick it up and displace it by several inches or to pass it to a friend; hereafter, tool transport) or use it (i.e., interacting with the object to functionally grasp it and use it). After 12 s the planning cue was replaced with the word "GO" for 6 s, during which time the participants generated a tool-directed gesture while the word remained on the screen.

Trial events were interspersed by 18-s rest periods in which a fixation cross was presented centrally with the word "FIXATE" positioned in the same physical location as the cues during the experimental trials. During these fixation events participants were instructed to relax and to wait for the next trial. We used the 18-s interstimulus period to temporally separate the principal events in the experiment for subsequent functional connectivity analyses, and to separately quantify functional connectivity in the absence of the experimental stimuli (i.e., during a baseline fixation period). As described below, this approach permits us to measure the modulation of functional connectivity maximally driven by tool use planning and pantomiming in relation to tool transport planning and pantomiming, over and above functional connectivity observed during this baseline period (i.e., a two-way functional connectivity interaction; for a similar experimental design and analysis pipeline, see Garcea et al., 2018; for a recent review on this technique, see Gonzalez-Castillo & Bandettini, 2017).

Prior to the scan, careful training and instruction was given to participants to pantomime tool use and tool transport actions. The training procedure was identical to previous training instructions we have administered to participants (e.g., Chen et al., 2016, 2017; Chen, Garcea, et al., 2018; Erdogan, Chen, Garcea, Mahon, & Jacobs, 2016; Garcea et al., 2018) in which participants are trained to generate a gesture as if the tool stimulus was "in-hand." Importantly, because participants are in a physically constrained environment in the bore of the magnet, they were instructed to generate gestures at a slow rate (~1 gesture per second) for the duration of the event; because there was no visual feedback during scanning (i.e., each participant's right hand was out of sight during the scan), the experimenter ensured that the participants memorized the tool transport and tool use actions prior to the scan by asking them to generate each action from memory. During each run the experimenter visually inspected the participant's gesturing action in real time to verify that the participants were generating actions when cued by the experiment. Participants were given feedback between runs to ensure tool use and tool transport actions were gestured correctly and with minimal inadvertent head movement.

2.4 | MR acquisition parameters

2.4.1 | MRI parameters

Whole brain BOLD imaging was conducted on a Siemens 3-Tesla PRISMA scanner with a 64-channel head coil located at the Hospital of the University of Pennsylvania. High-resolution structural T1 contrast images were acquired using a magnetization-prepared rapid gradient echo (MP-RAGE) pulse sequence at the start of each participant's scanning session (*TR* = 1850 ms, *TE* = 3.91 ms, flip angle = 8°, FOV = 256 mm, matrix = 256 × 192, 160 left-to-right slices, voxel size = 1 × 0.94 × 0.94 mm). An echo-planar imaging pulse sequence was used for T2* contrast (TR = 3,000 ms, TE = 30 ms, flip angle = 90°, FOV = 192 × 192 mm, matrix = 64 × 64, 48 inferior-to-superior slices, voxel size = 3 × 3 × 3 mm). Due to an error in image acquisition, two participants' data were acquired using a multi-echo sequence (*TR* = 3,000 ms, *TE* = 14 ms, flip angle = 90°, FOV = 216 × 216 mm, matrix = 68 × 68, 43 inferior-to-superior slices, voxel size = 3.17 × 3.17 × 3.5 mm). This acquisition procedure generated 3 dicoms per volume; the second dicom in each volume corresponds to the BOLD component of the MR signal (Kundu et al., 2013; Kundu, Inati, Evans, Luh, & Bandettini, 2012), and thus we included only those dicoms in subsequent analyses. Importantly, the results reported below do not change qualitatively when removing the two participants' data, therefore we include the two participants in all analyses. The first six volumes of each run were discarded to allow for signal equilibration (four volumes during image acquisition and two at preprocessing).

2.4.2 | Preprocessing of fMRI data

fMRI data were analyzed with the BrainVoyager software package (Version 2.8.2) and in-house scripts drawing on the BVQX toolbox written in MATLAB (http://support.brainvoyager.com/available-tools/52-matlab-tools-bvxqtools/232-getting-started.html). Preprocessing of the functional data included, in the following order, slice scan time correction (sinc interpolation), 3D motion correction with respect to the first volume of the first functional run, and linear trend removal in the temporal domain (cutoff: two cycles within the run). Functional data were registered (after contrast inversion of the first volume) to high-resolution deskulled anatomy on a participant-by-participant basis in native space. For each participant, echo-planar and anatomical volumes were transformed into standardized space (Talairach & Tournoux, 1988). All functional data were smoothed at 6 mm FWHM (two voxels). The general linear model (GLM) was used to fit beta estimates to the experimental events of interest. Experimental events were convolved with a standard 2-gamma hemodynamic response function. The first derivatives of 3D motion correction from each run were added to all models as regressors of no interest to attract variance attributable to head movement.

2.4.3 | Whole-brain BOLD contrast of tool use and tool transport viewing and planning

Upon completing the preprocessing steps described above, a group-level GLM was created with the 33 participants' data (i.e., random effects GLM). We began by computing the simple effect of task (two levels; viewing, planning) separately for tool use and tool transport trials. Given previous literature demonstrating increased BOLD contrast in frontoparietal action circuits when viewing images of manipulable objects (e.g., see Chao & Martin, 2000; Mahon et al., 2007), our goal was to isolate regions that exhibited increased BOLD contrast for action planning over and above tool viewing, and to determine where the effect was differentially modulated by tool use relative to tool transport. Thus we carried out the BOLD contrast analysis to replicate previous findings (Brandi et al., 2014) and we sought to extend those findings by demonstrating that the effect was present in the planning phase of a tool use action. In subsequent analyses we collapse across planning and pantomiming when computing whole-brain functional connectivity; we return to this issue below.

To measure the differential effect of tool use planning relative to tool transport planning, and to demonstrate the specificity of the planning effect over and above tool viewing, we computed a voxelwise directional interaction analysis using the contrast "[$\text{Planning}_{\text{Tool use}} - \text{Viewing}_{\text{Tool use}}$] − [$\text{Planning}_{\text{Tool transport}} - \text{Viewing}_{\text{Tool transport}}$]." Thus, any differential changes in the BOLD signal would be driven by planning tool use actions relative to planning tool transport actions, over and above the tool viewing condition which preceded the planning phase. The contrast was computed on a participant-by-participant basis, and a whole-brain one-sample *t*-test against 0 was computed to determine at the group-level which voxels exhibited significant differential BOLD contrast for tool use planning (positive *t*-values) and tool transport planning (negative *t*-values). This analysis identified five regions-of-interest (ROI) that were entered in a subsequent functional connectivity analysis: (a) the left SMG, (b) the left middle temporal gyrus, (c) the left frontal cortex (including the inferior and middle frontal gyri), (d) the left anterior insula, and (e) the left posterior insula extending laterally to include the left ventral premotor cortex (see Figure 2ai; see also Figure 3).

2.4.4 | Ensuring Independence of ROI selection from ROI testing

We took deliberate care to ensure that our results were statistically robust and independent. We selected ROIs for subsequent functional connectivity analyses using three approaches: (a) Using a leave-one-out approach to define the *N*th participant's ROIs with $N - 1$ participants' data, iterating this procedure across participants to define each ROI independently (e.g., see Kriegeskorte, Simmons, Bellgowan, & Baker, 2009); (b) Using literature-defined ROIs from previously published fMRI research on tool representation and action (e.g., see Anzellotti et al., 2011; Cant & Goodale, 2007; Q. Chen et al., 2016; Gallivan et al., 2013; Garcea et al., 2018); and (c) Using the Neurosynth database (http://neurosynth.org).

The left SMG, left middle temporal gyrus, left frontal cortex (inferior and middle frontal gyri), left anterior insula, and left posterior insula/ventral premotor cortex exhibited differential BOLD contrast for tool use planning from the interaction analysis, and we used a leave-one-out approach to define those regions on a participant-by-participant basis.

In a complementary approach using literature-defined regions, we selected four ROIs previously published by Gallivan et al. (2013), including the left posterior IPS, left posterior middle temporal gyrus, left SMG, and left ventral premotor cortex. These regions were shown to encode information about reaching-to-touch or reaching-to-grasp

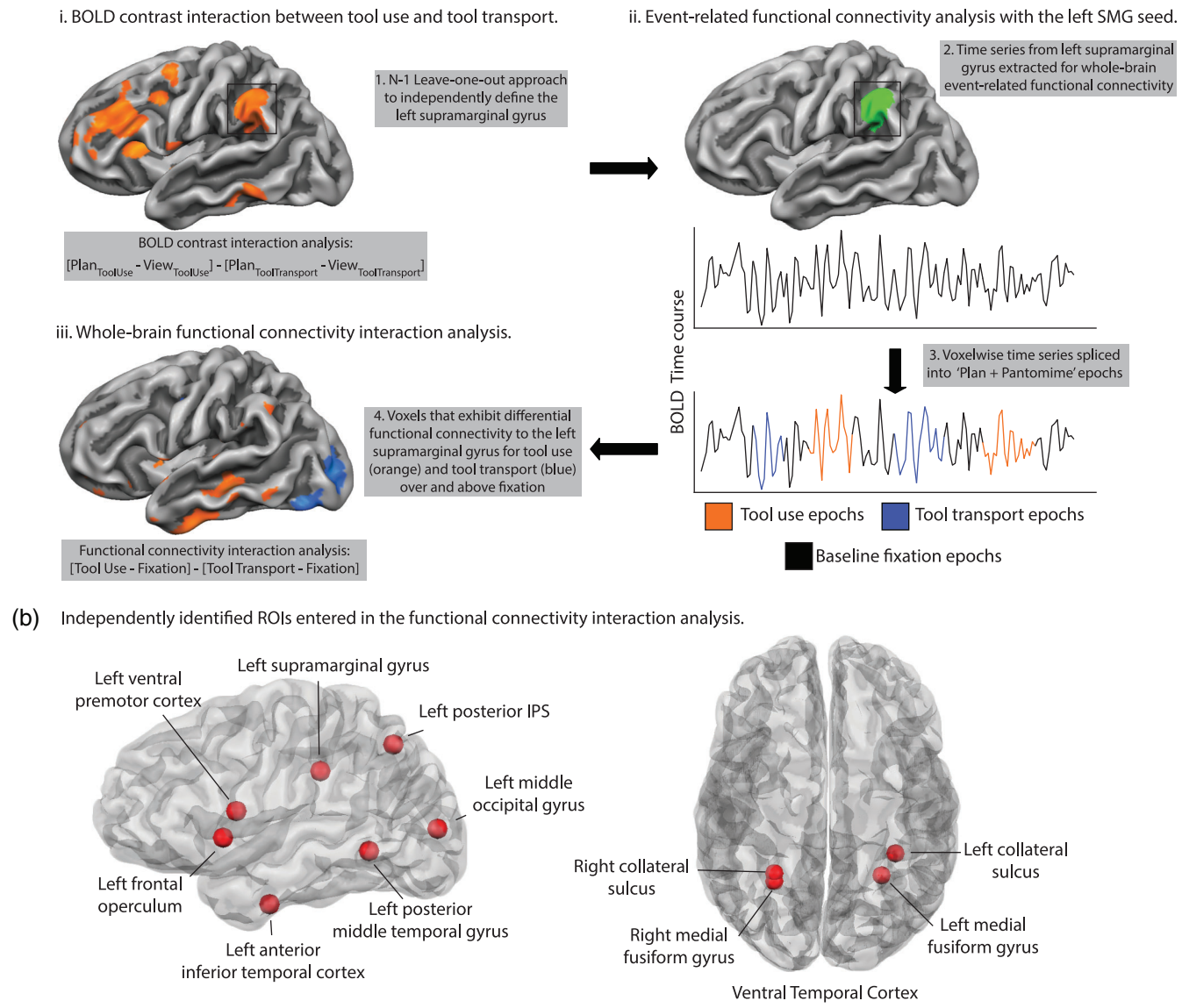

FIGURE 2 Task-based functional connectivity processing pipeline and independent literature-defined ROIs entered in the two-way functional connectivity interaction analysis (a). (i) Using an $N - 1$ leave-one-out approach, we identified regions-of-interest (ROI) using 32 participants' data to compute the directional two-way interaction between tool use and tool transport epochs, and iterated this procedure 33 times to define participant-specific left SMG spherical seed regions (10 mm in diameter) centered on the peak voxel. Next (ii), we extracted the time series from each participant's left SMG seed region and spliced the time series into the task-based portions of the experiment (functional volumes associated with planning and executing tool pantomiming) and the fixation baseline periods that followed each trial. We then computed a whole-brain functional connectivity map for the left SMG seed region separately for tool use and tool transport epochs and for fixation baseline periods that followed those epochs. We next performed a whole-brain functional connectivity interaction analysis that identified where functional connectivity was differentially modulated by tool use epochs relative to tool transport epochs, over and above the baseline fixation periods (iii). (b). We repeated the functional connectivity analysis using independently defined ROIs from prior studies focusing on tool planning and use. We used four regions from Gallivan et al. (2013), including the left SMG, left posterior IPS, left posterior middle temporal gyrus, and left ventral premotor cortex. We used the left and right collateral sulcus regions reported by Cant and Goodale (2007). We used a left anterior temporal lobe region reported by Anzellotti et al. (2011). We used bilateral medial fusiform gyri using peaks reported by Chen et al. (2016), and the left dorsal middle occipital gyrus using a peak reported by Garcea et al. (2018). Finally, we used the search term "left frontal operculum" on Neurosynth to define a peak in the left frontal operculum/inferior frontal gyrus

actions. Next, we selected the right and left medial fusiform gyri previously published by Chen et al. (2016), and the left dorsal occipital cortex (hereafter, left middle occipital gyrus) published by Garcea et al. (2018); both bilateral medial fusiform gyri and the middle occipital gyrus were shown to exhibit differential BOLD contrast for tool viewing relative to animal viewing. We used the right and left collateral sulci (published by Cant & Goodale, 2007), two regions that responded more strongly to surface texture than to orientation or object form, and we used a tool-preferring region in the left ventral anterior temporal lobe published in Anzellotti et al. (2011). Finally, we used the Neurosynth fMRI database to define the left IFG/frontal operculum using the search term "frontal operculum." Using the Harvard-Oxford cortical structural atlas in FSL we verified that the peak region was situated in left pars opercularis

TABLE 1 Peak Talairach coordinates from the BOLD contrast-defined and literature-defined regions of interest entered in the functional connectivity interaction analysis

Source of peak voxel coordinates	Peak Talairach coordinates		
	X	*Y*	*Z*
Gallivan et al. (2013)			
Left posterior Intraparietal sulcus	−22	−68	45
Left posterior middle temporal Gyrus	−53	−57	−3
Left supramarginal gyrus	−56	−35	33
Left ventral premotor cortex	−52	3	15
Chen et al. (2016)			
Left medial fusiform Gyrus	−27	−53	−13
Right medial fusiform Gyrus	27	−52	−14
Cant and Goodale (2007)			
Left collateral sulcus	−37	−42	−15
Right collateral sulcus	27	−56	−13
Garcea et al. *(2018)*			
Left dorsal occipital cortex	−31	−88	7
Anzellotti et al. *(2011)*			
Left anterior temporal lobe	−52	−12	−27
Neurosynth-defined region			
Left inferior frontal gyrus/frontal operculum	−49	9	3
BOLD contrast-defined regions			
Left supramarginal gyrus	−54	−37	37
Left frontal cortex	−51	23	25
Left middle temporal gyrus	−63	−40	−8
Left anterior insula	−30	17	13
Left posterior insula	−39	−4	1

(Brodmann Area 44), and we converted the peak MNI coordinate to Talairach space for subsequent analyses.

As outlined in the introduction, we selected these 11 regions because they represent a literature that has focused on the processing of tools and their associated actions from the perspective of object processing in the ventral visual pathway, sensory-motor processing in the dorsal visual pathway, and selection mechanisms supported by prefrontal and premotor regions. For all regions entered into the functional connectivity analysis, we created a spherical ROI 10 mm in diameter centered on each participant-specific, literature-defined, and Neurosynth-defined peak coordinate (see Table 1 for peak Talairach coordinates). Thus all ROIs were on equal footing with respect to the number of voxels in each sphere.

2.4.5 | The modulation of functional connectivity by the interaction of task and action type

The principal focus of the analysis was to measure the degree to which functional connectivity was modulated by the interaction of Task (two levels; plan + pantomime, fixation) and action type (two levels; tool use, tool transport). We modeled functional connectivity for the planning and pantomiming phase as one condition for three reasons: (a) The planning phase of our task was too short in duration (12 s, four volumes) to compute functional connectivity in isolation (i.e., there is an increased risk of committing Type I error when computing functional connectivity over a shorter duration); (b) Because pantomiming epochs followed planning epochs closely in time, we were unable to separate functional connectivity driven by planning processes from functional connectivity driven by pantomiming processes; (c) The hand posture required to generate a tool transport gesture was more homogeneous across actions than tool use actions. For these reasons we modeled both events together into a "plan + pantomime" epoch, and we used an identical analytic approach as was carried out by Garcea et al. (2018) to measure where functional connectivity was differentially modulated for tool use epochs relative to tool transport epochs, over and above functional connectivity measured during fixation epochs (see Figure 2a). Prior to computing functional connectivity, the change in head position (translation and rotation in *XYZ* dimensions) across volumes was regressed out of the time series data (after the preprocessing steps described above); all functional connectivity analyses were conducted over the residuals of that regression model. We did not regress the global mean time course, as work has suggested that this procedure is at best unnecessary, and at worst may introduce spurious correlation patterns to the data (e.g., see Gotts, Jo, et al., 2013; Gotts, Saad, et al., 2013; Saad et al., 2013).

To measure the differential modulation of functional connectivity, we extracted the BOLD time series data that corresponded to trial events for tool use and tool transport epochs, and separately, for the fixation event portion of the BOLD time series that immediately followed each trial (see Figure 2aii). We extracted six volumes (18 s) of time series data aligned to the onset of each plan type (four volumes) and the subsequent pantomime event (two volumes). There were eight trials presented in each run; thus, we derived eight 6-volume-long time series segments for each run and correlated the time series data extracted from a given ROI for those volumes with the time series data for those volumes in every other voxel of the brain. Functional connectivity was computed with the NeuroElf toolbox (https://neuroelf.net) in MATLAB using the "vtc_CrossCorrelate" function. The functional connectivity analysis resulted in eight whole-brain functional connectivity maps per run. We then Fisher-transformed each functional connectivity map and averaged together the eight whole-brain maps for tool use planning and pantomiming (four maps from Run 1; four maps from Run 2) and the eight whole-brain maps for tool transport planning and pantomiming. In a manner identical to the analysis of tool use and tool transport events described above, we computed whole-brain functional connectivity during the poststimulus fixation events and averaged together the fixation baseline maps separately for events that followed tool use epochs and tool transport epochs. See Figure 2a for a schematic of the two-way functional connectivity analysis.

This procedure resulted in four whole-brain maps per participant, which were entered in a two-way interaction analysis to determine where functional connectivity was differentially modulated by tool use planning and pantomiming in relation to tool transport planning and pantomiming, over and above modulation in functional connectivity observed during fixation events "[Tool $use_{plan\ +\ pantomime}$ − Fixation $_{tool\ use}$] − [Tool $transport_{plan\ +\ pantomime}$ − $Fixation_{tool\ transport}$]." We then computed a one-sample *t*-test against 0 in each voxel to determine the extent to which the directional two-way functional connectivity interaction

was differentially modulated by tool use planning and acting (positive *t*-values) and tool transport planning and acting (negative *t*-values) across participants (see Figure 2aiii).

We took two approaches to interpreting functional connectivity. First, we used the left SMG region derived from the BOLD contrast interaction analysis as a seed, and we used the remaining regions (i.e., left middle temporal gyrus, left frontal cortex, left anterior insula, left posterior insula/ventral premotor) as mask regions from which to extract functional connectivity for interpretation. In a parallel analysis, we use 11 independently defined regions from the tool and action literature reviewed above to serve as seed and mask regions, and we tested for functional connectivity modulations differentially driven by tool use actions relative to tool transport actions (see Figure 2b).

3 | RESULTS

3.1 | BOLD contrast analysis of planning tool use and tool transport actions

There were four factors in our design that were directly contrasted in the BOLD analysis: Task type (two levels; view, plan) and Action type (two levels; tool use, tool transport). We began by testing the directional interaction between task type separately for tool use ($[Plan_{Tool\ use} - View_{Tool\ use}]$) and tool transport ($[Plan_{Tool\ transport} - View_{Tool\ transport}]$) actions. We then directly contrasted tool use planning against tool transport planning ($[Plan_{Tool\ use} - View_{Tool\ use}] - [Plan_{Tool\ transport} - View_{Tool\ transport}]$) to determine the anatomical loci differentially engaged by planning tool use or tool transport actions.

3.1.1 | Simple effect: Tool use planning

The whole-brain contrast of tool use planning against tool viewing is plotted in Figure 3a. All voxels plotted survive FDR correction ($q < 0.05$). Relative to tool viewing, tool use planning elicited increased BOLD contrast across a swath of cortical and subcortical regions, including bilateral supramarginal gyri, the left superior parietal lobule, bilateral ventral premotor cortex extending medially into the insula and adjacent subcortical voxels in the vicinity of the basal ganglia, bilateral middle frontal gyri extending superiorly into the superior frontal gyri, and bilateral dorsal premotor cortex ending medially into the supplementary motor area. A contiguous cluster of voxels not pictured on the cortical rendering was identified in the left superior pre- and postcentral gyrus. In contrast, tool viewing during the use epochs elicited increased BOLD contrast in bilateral ventral temporal cortex, including bilateral inferior temporal gyri and medial fusiform gyri, extending anteriorly into the anterior ventral temporal lobe. Superior parietal-occipital cortices also exhibited increased BOLD contrast for tool viewing (see Table 2a for peak voxel coordinates and *t*-values associated with the tool use contrast map).

3.1.2 | Simple effect: Tool transport planning

The whole-brain contrast of tool transport planning against tool viewing is plotted in Figure 3b. All voxels plotted survive FDR correction ($q < 0.05$). We observed qualitatively similar results as was observed for tool use planning, albeit quantitatively weaker for tool transport planning. Relative to tool viewing, tool transport planning elicited increased BOLD contrast in the right SMG, in the left superior parietal lobule, in the left dorsal premotor cortex extending medially into the left supplementary motor area, in the medial aspect of the left and right IFG adjacent to the insula, and in bilateral putamen. Relative to tool transport planning, tool viewing in the transport epochs elicited a pattern of BOLD contrast virtually identical to the contrast map in Figure 3a. Specifically, we observed robust increase in BOLD contrast in bilateral inferior temporal gyri and medial fusiform gyri, which extended anteriorly into the anterior and ventral temporal lobe; in addition, we observed increased BOLD contrast in bilateral superior parietal-occipital cortices (see Figure 3b and Table 2b for peak voxel coordinates and *t*-values associated with the tool transport contrast map).

3.1.3 | Interaction between task and action type

Next, we directly contrasted tool use planning against tool transport planning using a whole-brain directional two-way interaction analysis. Specifically, we computed at the voxel level the degree to which BOLD contrast was differentially modulated by tool use planning relative to tool transport planning, over and above changes observed for viewing. We found five left hemisphere cortical clusters that exhibited a preference for tool use planning: (a) the left SMG, (b) the left middle temporal gyrus, (c) the left frontal cortex (including the inferior and middle frontal gyrus), (d) the left anterior insula, and (e) the left posterior insula extending laterally to the left ventral premotor cortex (see Figure 3c). Consistent with Brandi et al. (2014), we find no left hemisphere cortical voxels that exhibit a differential BOLD response for tool transport relative to tool use (but see Supporting Information Figure S1). In a supplemental analysis, we modeled the gesturing phase in isolation from the planning phase when contrasting tool use against tool transport, and we observed results for tool use gesturing that were qualitatively similar to those displayed in Figure 3c (see Supporting Information Figure S1).

It is important to note that the left middle temporal gyrus peak here (peak: −63 −40 −8) is anterior to the oft-reported left posterior middle temporal gyrus locus identified in previous tool use fMRI studies in neurotypical adults (Chen et al., 2016; Gallivan et al., 2013; Garcea & Mahon, 2014) and in neuropsychological populations (Campanella, D'Agostini, Skrap, & Shallice, 2010; Kalenine & Buxbaum, 2016). To address this anatomical discrepancy we include a literature-defined left posterior middle temporal gyrus in our functional connectivity analyses (see below).

3.2 | Modulation of functional connectivity by the interaction of task and action type

3.2.1 | Interaction analysis with BOLD contrast-defined regions

Next, we sought to determine whether the left SMG exhibits increased functional connectivity for tool use planning and pantomiming relative to tool transport planning and pantomiming, over and above fixation baseline functional connectivity, to the regions identified in the BOLD contrast analysis. We observed increased functional connectivity to the left middle temporal gyrus for tool use epochs (relative to fixation baseline; $t(32) = 5.36$, $p < 0.001$) and for tool transport epochs (relative to fixation baseline; ($t(32) = 4.28$, $p < 0.001$); this

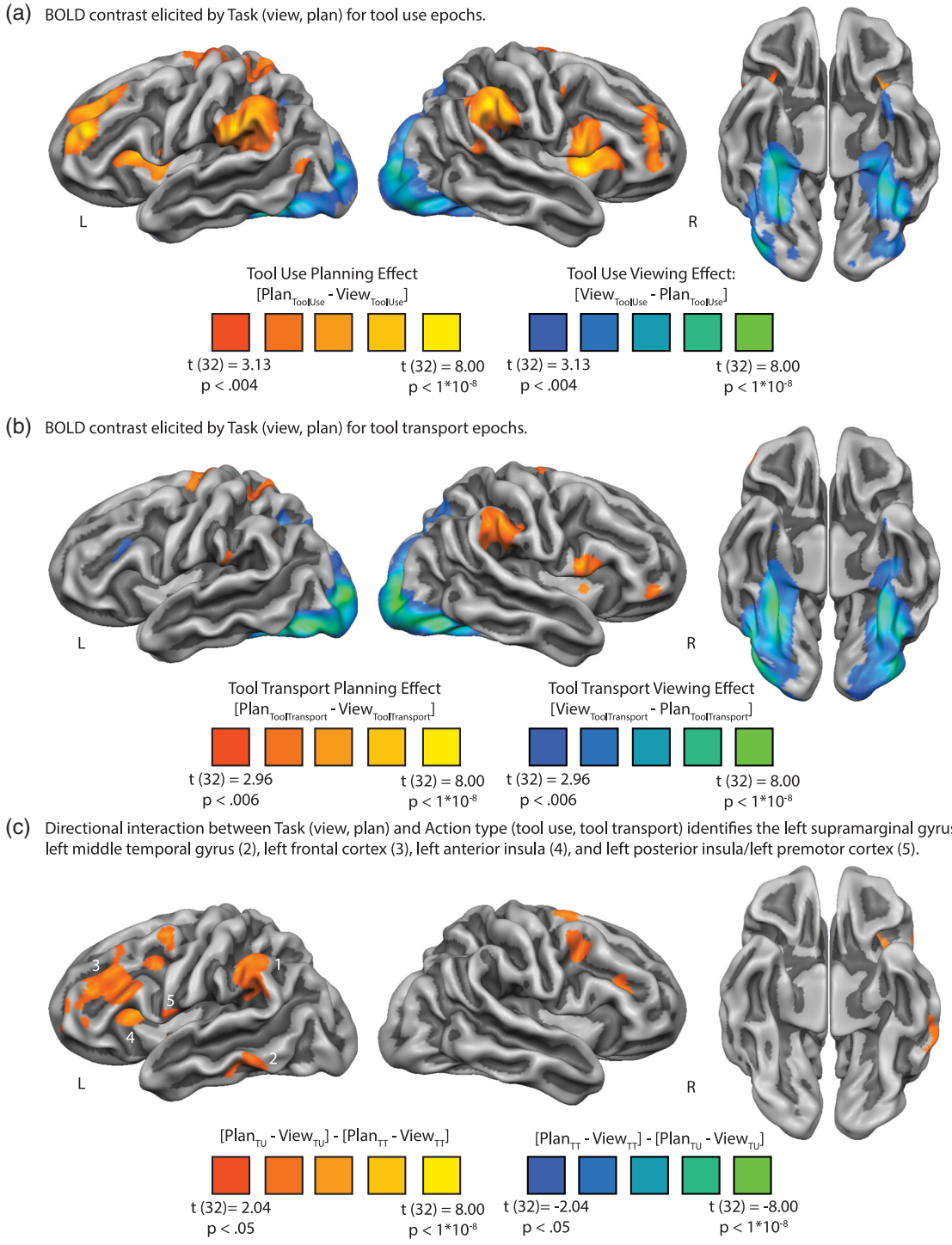

FIGURE 3 BOLD contrast interaction analysis identifies a swath of left hemisphere regions involved in tool use planning. (a) Whole-brain BOLD response elicited by task (view, plan) for tool use epochs. Tool use planning elicited increased BOLD contrast in the left and right supramarginal gyri, left superior parietal lobule, left ventral premotor cortex, bilateral insula and inferior frontal gyri, and bilateral dorsolateral prefrontal cortices. In contrast, tool viewing elicited increased BOLD contrast bilaterally in posterior parietal/dorsal occipital cortices, bilateral inferior temporal gyri, and bilateral medial fusiform gyri extending anteriorly into the parahippocampal gyri and anterior temporal lobes. (b) Whole-brain BOLD response elicited by task (view, plan) for tool transport trials. Relative to tool viewing, tool transport epochs elicited increased BOLD contrast in bilateral supramarginal gyri, the left superior parietal lobule, and bilateral dorsal premotor cortices extending medially to the supplementary motor area. In contrast to tool transport epochs, tool viewing elicited increased BOLD contrast in bilateral posterior parietal and dorsal occipital cortices, inferior temporal gyri, medial fusiform gyri, and anterior temporal lobes. Data in panels (a) and (b) survive FDR correction ($q < 0.05$). (c) the whole-brain interaction between task (view, plan) and action type (tool use, tool transport) identifies the left SMG, left middle temporal gyrus, left frontal cortex, left anterior insula, and left posterior insula extending laterally to the left ventral premotor cortex as exhibiting differential BOLD contrast for tool use epochs relative to tool transport epochs, over and above BOLD contrast for tool viewing. Note that all regions survive cluster correction of 40 contiguous voxels; the left inferior parietal lobule and left middle frontal gyrus survive cluster-correction when using a more restrictive threshold (cluster correction using AlphaSim, minimum cluster size of 123 voxels, with an alpha value of $p < 0.05$)

TABLE 2 Peak Talairach coordinates, maximum t-value, cluster size, and anatomical region for the BOLD contrast analysis reported in Figure 3

Region name	Peak Talairach coordinates			Maximum *t*-value	Anatomical voxels (1 mm^3)
	X	*Y*	*Z*		
A. Tool use planning > tool viewing					
Left middle frontal gyrus	−30	44	25	$t(32) = 6.91, p < 0.001$	8,633
Right supramarginal gyrus	51	−37	−37	$t(32) = 6.75, p < 0.001$	11,391
Right putamen	24	−1	13	$t(32) = 6.60, p < 0.001$	15,146
Left supramarginal gyrus	−57	−31	25	$t(32) = 6.26, p < 0.001$	36,439
Right middle frontal gyrus	33	44	34	$t(32) = 6.26, p < 0.001$	8,222
Left putamen	−24	−7	13	$t(32) = 6.12, p < 0.001$	12,759
Left cerebellum	−33	−37	−35	$t(32) = 4.84, p < 0.001$	2,815
Left precentral gyrus	−52	2	43	$t(32) = 4.57, p < 0.001$	877
Right cerebellum	39	−37	−38	$t(32) = 4.22, p < 0.001$	475
Left posterior middle temporal gyrus	−45	−64	7	$t(32) = 4.02, p < 0.001$	452
Right prefrontal cortex	24	59	3	$t(32) = 3.64, p < 0.001$	326
Right medial fusiform gyrus	27	−58	−11	$t(32) = -7.93, p < 0.001$	44,555
Left medial fusiform gyrus	−33	−46	−14	$t(32) = -7.53, p < 0.001$	26,835
Right cingulate cortex	−9	−25	28	$t(32) = -4.67, p < 0.001$	1,289
Left anterior temporal lobe	−27	8	*−29*	$t(32) = -4.58, p < 0.001$	1,375
B. Tool transport planning > tool viewing					
Left putamen	−27	−7	1	$t(32) = 6.18, p < 0.001$	1926
Left somatosensory cortex	−21	−19	64	$t(32) = 5.53, p < 0.001$	7,779
Right supramarginal gyrus	60	−34	37	$t(32) = 4.76, p < 0.001$	4,875
Right inferior frontal gyrus	51	8	13	$t(32) = 4.67, p < 0.001$	3,538
Right prefrontal cortex	45	41	1	$t(32) = 4.55, p < 0.001$	834
Right putamen	24	−7	7	$t(32) = 4.52, p < 0.001$	614
Left anterior cingulate cortex	−12	44	16	$t(32) = 4.16, p < 0.001$	516
Left supramarginal gyrus	−54	−28	22	$t(32) = 3.95, p < 0.001$	529
Right middle occipital gyrus	30	−82	2	$t(32) = -10.58, p < 0.001$	49,959
Left middle occipital gyrus	−27	−88	4	$t(32) = -9.23, p < 0.001$	43,292
Right thalamus	18	−28	−3	$t(32) = -4.55, p < 0.001$	494
Left middle/inferior frontal gyrus	−39	20	25	$t(32) = -3.86, p < 0.001$	798

increase in functional connectivity for tool use epochs was not significantly stronger than tool transport epochs ($t(32) = 1.30$, $p = 0.20$; see Supporting Information Figure S2).[2] A similar pattern was present when measuring functional connectivity to the left frontal cortex ROI: we found increased functional connectivity for tool use epochs ($t(32) = 3.62$, $p < 0.001$) and tool transport epochs ($t(32) = 3.51$, $p < 0.001$) relative to baseline; however, the interaction was not significant ($t < 1$). Lastly, there was no differential functional connectivity to the left anterior insula or to the left posterior insula ROIs (all *t*-values <1; see Supporting Information Figure S2c).

3.2.2 | Interaction analysis with independently-defined regions

Next, we used the same analytic approach with our independent literature-defined and Neurosynth-defined ROIs to determine the extent to which functional connectivity among the 11 regions was differentially driven by tool use and tool transport epochs. The analysis proceeded in two steps. In the first step, we used each ROI as a seed region to compute whole-brain functional connectivity, and we used the ten remaining regions as masks to extract functional connectivity values; this resulted in an 11-by-11 two-way interaction matrix. In the second step, we interpreted the significance of the data if the observed functional connectivity values satisfied three constraints: (a) functional connectivity must be significant bi-directionally (e.g., when using region A as a seed and region B as a mask, and vice versa), (b) at an alpha level of at least $p < 0.01$, and (c) the effect size for the two-way interaction must be moderate in magnitude (Hedges' G of 0.40 or higher). After imposing those constraints we found seven significant ROI-to-ROI effects: For tool use epochs, we observed a significant two-way interaction between the left SMG and (a) the left ventral anterior temporal lobe and (b) the left frontal operculum/IFG (see Figure 4a,b); for tool transport epochs, we observed a significant two-way interaction between the left SMG and (c) right collateral sulcus, (d) the left medial fusiform gyrus, (e) the right medial fusiform gyrus, (f) the left middle occipital gyrus, and (g) between the left middle occipital gyrus and left posterior middle temporal gyrus (see Figure 4b). Functional connectivity that was bi-directionally robust but did not survive a *p* value cutoff of 0.01 is

[2]When using a more restrictive statistical threshold to define the left middle temporal gyrus peak, we replicated the significant increase in functional connectivity for tool use (relative to fixation baseline; $t(32) = 7.04$, $p < 0.001$) and tool transport epochs (relative to fixation baseline; ($t(32) = 3.75$, $p < 0.001$), and we found that the increase in functional connectivity for tool use epochs was differentially stronger than tool transport epochs ($t(32) = 2.28$, $p < 0.05$; i.e., a significant two-way interaction).

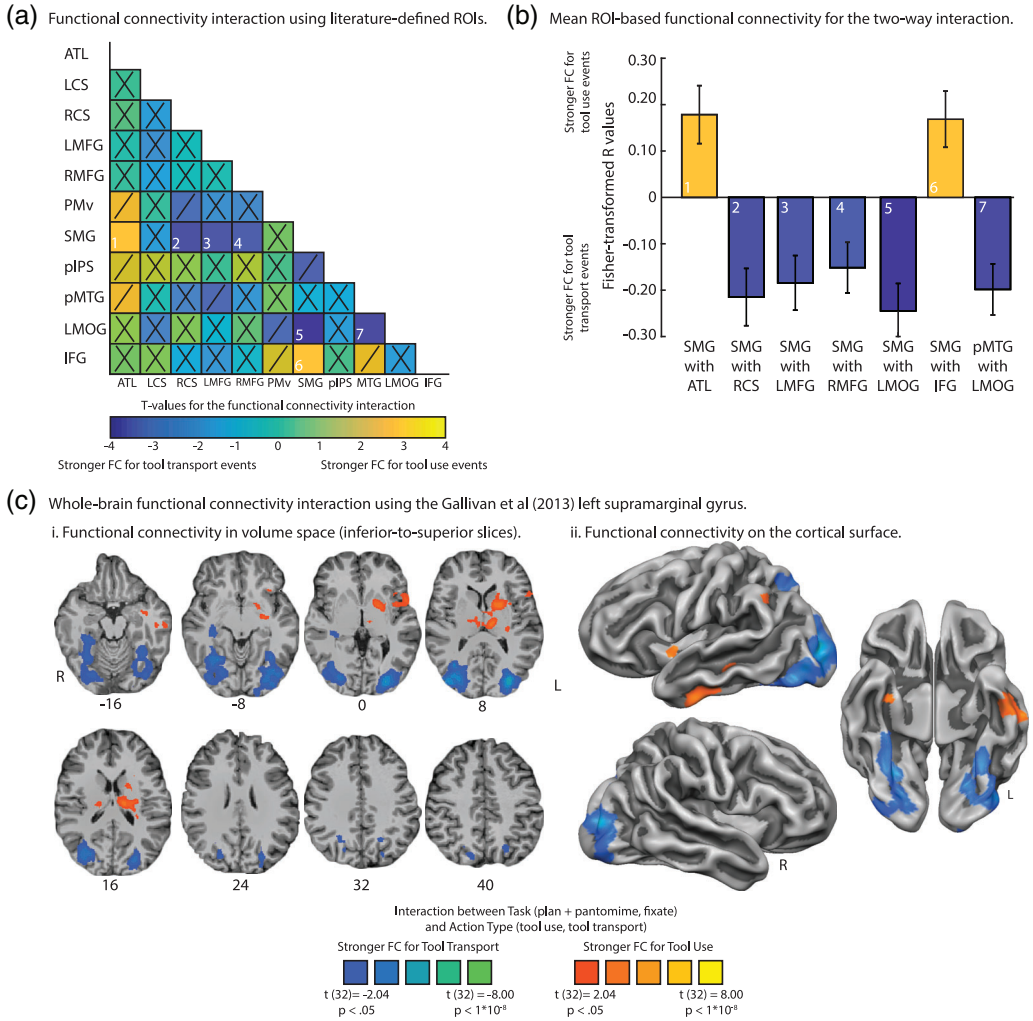

FIGURE 4 Modulation of functional connectivity for the interaction between task and action type. (a) ROI-based functional connectivity interaction analysis between task (task-based functional connectivity, fixation baseline functional connectivity) and action type (tool use, tool transport) using independently defined seed regions. We quantified the degree to which functional connectivity was differentially driven by tool use planning and pantomiming epochs (hot colors) relative to tool transport planning and pantomiming epochs (cold colors) over and above changes in functional connectivity observed during baseline fixation events. We report significant effects if the two-way modulation in functional connectivity satisfied three constraints: (i) functional connectivity must be significant bi-directionally (e.g., when using region A as a seed and region B as a mask, and vice versa), (ii) at an alpha level of at least $p < 0.01$, and (iii) the effect size for the two-way interaction must be moderate in magnitude (Hedges' G of 0.40 or higher). Functional connectivity that was bi-directionally present but that did not survive p-value correction (i.e., $p < 0.05$, uncorrected) is marked with a "/"; functional connectivity that was not significant is marked with an "X." For tool use epochs, there was increased functional connectivity between the left SMG and left ventral anterior temporal lobe, and between the left SMG and left frontal operculum/inferior frontal gyrus. For tool transport epochs, we found increased functional connectivity between the left SMG and right collateral sulcus, left SMG and bilateral medial fusiform gyri, left SMG and left middle occipital gyrus, and between the left posterior middle temporal gyrus and left middle occipital gyrus. (b) the average Fisher-transformed correlation coefficients associated with the two-way interaction are plotted; error bars reflect standard error of the mean across participants. (c) the whole-brain two-way interaction map for the left SMG seed from Gallivan et al. (2013) illustrates modulations associated with tool use and tool transport events, which are qualitatively similar to what was observed using the BOLD contrast-defined left SMG (see Supporting Information Figure S2 for whole-brain functional connectivity interaction map). All voxels survive cluster correction using AlphaSim (minimum cluster size of 125 voxels, with an initial alpha value of $p < 0.05$). Abbreviations. ATL, left anterior temporal lobe; IFG, left frontal operculum/left inferior frontal gyrus; LCS, left collateral sulcus; LMFG, left medial fusiform gyrus; LMOG, left middle occipital gyrus; pIPS, left posterior intraparietal sulcus; PMv, left ventral premotor cortex; pMTG, left posterior middle temporal gyrus; RCS, right collateral sulcus; RMFG, right medial fusiform gyrus; SMG, left supramarginal gyrus

marked with a "/"; all other nonsignificant functional connectivity is marked with a "X" (see Figure 4a; see also Table 3 for t-values and effect sizes associated with the two-way analysis; see Supporting Information Table S1 for the average group-level functional connectivity values and p-values).

Lastly, to confirm the results of the functional connectivity analysis using the BOLD contrast-defined left SMG, we projected the whole-brain two-way interaction map using the Gallivan et al. (2013) left SMG seed in volume space (Figure 4ci) and on the cortical surface (Figure 4cii). The resulting map confirms the ROI-based functional connectivity analysis: Tool use epochs elicited increased functional connectivity to the left anterior ventral temporal cortex ($Z = -16$), and to the left frontal operculum extending into the left posterior insula to include aspects of the basal ganglia ($Z = 0, 8$; for cluster-level analysis see

TABLE 3 t-values associated with the two-way interaction between task (plan + pantomime, fixate) and action type (tool use, tool transport)

	ATL	LCS	RCS	LMFG	RMFG	PMv	SMG	pIPS	pMTG	LMOG	IFG
ATL	–	–	–	–	–	*2.78*	3.13 (0.58)	–	*2.61*	–	–
LCS	–	–	–	–	–	–	–	–	–	–	–
RCS	–	–	–	–	–	*−2.22*	−3.50 (0.54)	–	–	–	–
LMFG	–	–	–	–	–	–	−2.86 (0.47)	–	*−2.14*	–	–
RMFG	–	–	–	–	–	–	−2.95 (0.46)	–	–	–	–
PMv	*2.46*	–	*−2.00*	–	–	–	–	–	–	–	–
SMG	2.86 (0.53)	–	−3.48 (0.57)	−3.12 (0.52)	−2.77 (0.41)	–	–	*−2.20*	–	−3.40 (0.60)	2.71 (0.63)
pIPS	–	–	–	–	–	–	*−2.62*	–	–	–	–
pMTG	*2.44*	–	–	*−2.29*	–	–	–	–	–	−3.08 (0.67)	*2.74*
LMOG	–	–	–	–	–	–	−4.13 (0.75)	–	−3.60 (0.76)	–	–
IFG	–	–	–	–	–	–	2.78 (0.67)	–	*2.35*	–	–

t-values are reported if they satisfy the joint constraint of reaching significance at $p < 0.01$ across data folds with an effect size (Hedge's *G*) that is moderate in magnitude (minimum value of 0.40); the magnitude of the effect size is given in parentheses. Functional connectivity values that do not meet those constraints but that are significant across data folds ($p < 0.05$) are listed in italics. Columns correspond to the seed regions and rows correspond to mask regions from which functional connectivity was extracted. Abbreviations. ATL, left anterior temporal lobe; LCS, left collateral sulcus; IFG, left frontal operculum/left inferior frontal gyrus; LMFG, left medial fusiform gyrus; LMOG, left middle occipital gyrus; RCS, right collateral sulcus; RMFG, right medial fusiform gyrus; pIPS, left posterior intraparietal sulcus; pMTG, left posterior middle temporal gyrus; PMv, left ventral premotor cortex; SMG, left supramarginal gyrus.

Table 4). In contrast, tool transport epochs elicited increased functional connectivity to a bilateral swath of cortex in ventral temporal cortex, including bilateral medial fusiform gyri extending into the collateral sulci (*Z* = −16), bilateral middle occipital gyri (*Z* = 0, 8), and posterior IPS extending into the superior parietal lobe (*Z* = 24, 32, 40; see Table 4; see also Supporting Information Figure 2a).

4 | GENERAL DISCUSSION

The 2AS+ model predicts that functional connectivity to the left SMG should be modulated by action tasks emphasizing diverse tool-directed computations. To assess that prediction, we conducted a task-based functional connectivity study in which neurotypical adult participants planned and pantomimed tool use and tool transport actions. We first demonstrated a greater engagement of the left SMG, left middle temporal gyrus, left frontal cortex, left anterior insula, and left posterior insula extending laterally into ventral premotor cortex for tool use planning relative to tool transport planning. Next, we modeled increases in functional connectivity separately for planning and pantomiming epochs for tool use versus transport, and contrasted the modulation in functional connectivity between those conditions over and above baseline levels of functional connectivity quantified during fixation events. We found strong increases in functional connectivity for tool use between the left SMG and left middle temporal gyrus, however the effect was only marginally stronger relative to tool transport. In a final series of analyses we computed functional connectivity among 11 literature-defined regions implicated in object processing, sensory-motor processing, and action selection. For tool use epochs there was increased functional connectivity between the left SMG and ventral anterior temporal lobe, as well as between the left SMG and IFG/frontal operculum; in contrast, for tool transport epochs there was increased functional connectivity between the left SMG and right collateral sulcus, left and right medial fusiform gyri, left middle occipital gyrus, and between the left posterior middle temporal gyrus and left middle occipital gyrus.

Our results demonstrate that functional interactions with the left SMG are differentially modulated by tool-directed pantomime actions emphasizing semantic or sensory-motor processing demands. Producing a tool use action, by hypothesis, presupposes the integration of conceptual knowledge of tools with knowledge of the appropriate posture of the fingers, hand, and joints required for skilled tool manipulation. In contrast, tool transport pantomiming bypasses semantic processing, and emphasizes the extraction of three-dimensional volumetric properties of a tool in the environment relative to the hand

TABLE 4 Peak Talairach coordinates, peak t-value, p-value, and cluster size for the two-way functional connectivity interaction reported in Figure 4c

	Peak Talairach coordinates				
Region name	***X***	***Y***	***Z***	**Peak *t*-value**	**Anatomical voxels (1 mm^3)**
Tool use > tool transport					
Left thalamus	−12	−16	10	$t(32) = 4.09$, $p < 0.001$	4,500
Left putamen	−18	5	7	$t(32) = 4.13$, $p < 0.001$	6,214
Left ventral inferior temporal gyrus	−45	−13	−23	$t(32) = 3.97$, $p < 0.001$	4,302
Tool transport > tool use					
Right middle occipital gyrus	39	−82	7	$t(32) = 5.23$, $p < 0.001$	27,981
Left middle occipital gyrus	−30	−79	4	$t(32) = 6.00$, $p < 0.001$	23,625

and body in order to displace or transport a tool several inches. In the sections below, we evaluate our findings in relation to prominent neurocognitive models of action production and tool use.

Our BOLD contrast results are consistent with previous studies demonstrating that the left SMG processes tool-associated manipulation knowledge (Boronat et al., 2005; Canessa et al., 2008; Johnson-Frey et al., 2005; Kellenbach et al., 2003; for discussion, see Orban & Caruana, 2014). For example, Brandi et al. (2014) found that generating tool use actions, relative to tool transport actions, elicited increased BOLD signal in the left SMG, lateral occipital complex (in the vicinity of the left posterior middle temporal gyrus) and ventral premotor cortex (among other areas). Moreover, we extend their findings by controlling for tool viewing; this is an important control, as prior research indicates that the left SMG, middle temporal gyrus, and ventral premotor cortex exhibit increased BOLD contrast for tool stimuli in passive viewing paradigms (Chao & Martin, 2000; Garcea et al., 2016; Garcea & Mahon, 2014; Grafton et al., 1997; Mahon et al., 2007; Noppeney et al., 2006).

One discrepancy between our results and previous findings relates to the difference between the left middle temporal gyrus identified in the BOLD contrast analysis and the literature-defined left posterior middle temporal gyrus. For example, although the peak of our BOLD contrast-defined left SMG was in good agreement with the Gallivan et al. (2013) peak (4.9 mm in Euclidean distance), our left middle temporal gyrus was 20.4 mm in Euclidean distance from the Gallivan et al. (2013) left posterior middle temporal gyrus peak. Nevertheless, there was strong functional connectivity for tool use epochs between our BOLD contrast-defined left SMG and left middle temporal gyrus, replicating prior work demonstrating these regions exhibit resting state connectivity (Simmons & Martin, 2012) and task-based functional connectivity driven by tool use (Garcea et al., 2018; Hutchison & Gallivan, 2018; Kleineberg et al., 2018). Future studies using participant-specific ROIs derived from independent localizer tasks will be able to resolve subtle differences in peak voxels used in functional connectivity analyses.

In our BOLD contrast analysis and ROI-based functional connectivity analysis the left IFG was identified as a region involved in tool use planning and pantomiming. Previously, we have provided evidence that the left IFG may provide a top-down biasing signal that resolves competition between candidate tool use actions, supported by functional connectivity with the left SMG (Buxbaum, 2017; see also Cisek & Kalaska, 2010). Other proposals argue that subregions within left IFG participate in distinct components of action, supported by separate white matter fiber tracts connected to the left inferior parietal lobule. For example, Hamzei et al. (2016) used fMRI to parcellate the left IFG into subregions that responded maximally when observing actions, imitating actions, or when grasping a tool without visual feedback. The investigators found that Brodmann area 44 dorsal (BA44d) responded maximally to action observation and imitation, whereas Brodmann Area 44 ventral (BA44v; approximately 4.4 mm in Euclidean distance from our Neurosynth-defined IFG/frontal operculum ROI) responded maximally when grasping a tool without visual feedback. Follow-up diffusion tractography analyses identified white matter connectivity between BA44d and the left inferior parietal lobule via the superior longitudinal fasciculus (SLF; dorsal route), whereas ventral Area 44 (BA44v) and the left inferior parietal lobule were connected via the extreme capsule (ventral route). Consistent with these findings, Vry et al. (2015) identified the extreme capsule as connecting regions involved in pantomiming tool use, including pars triangularis of the left IFG, the left middle temporal gyrus, and the left inferior parietal regions (SMG, IPS); in contrast, frontal and parietal regions involved in imitation of object use and imitation of meaningless gestures were connected by the dorsal route, principally via the SLF. On the other hand, our own prior research has identified the SLF as critical to error-free pantomime production in patients with stroke (e.g., see Watson & Buxbaum, 2015). Thus, an area of continued interest for future work is the extent to which subregions of left prefrontal cortex integrate distinct aspects of action supported via the ventro-dorsal stream, and the ventral (extreme capsule) and dorsal (SLF) fiber tracts reported by Vry et al. (2015) and Hamzei et al. (2016).

We also found strong functional connectivity between the left SMG and left ventral anterior temporal lobe for tool use actions (see Figure 4). Prior TMS studies have found that repetitive stimulation to the left ventral anterior temporal lobe selectively slowed down function judgments of tools, but had no effect on response time when participants made manipulation judgments of tools (Andres et al., 2013; Ishibashi et al., 2011; for discussion, see Garcea & Mahon, in press). Comparable findings in the fMRI literature have been reported by Chen and colleagues (Chen et al., 2016; Chen, Garcea, et al., 2018). For example, when participants were asked to generate tool use gestures to the visual presentation of objects, Chen et al. (2016) found that mesial and anterior temporal cortex encoded gestures that shared the same function or purpose of use (see also Canessa et al., 2008), whereas the left SMG encoded gestures that were similar in hand posture and tool use kinematics (see also Gallivan et al., 2013). As noted in the introduction, tool use planning and gesturing emphasizes the integration of semantic processing (including the processing of function knowledge) with skilled tool use action processes, which may be supported via the ventral white matter route proposed by Vry et al. (2015).

In contrast, planning and pantomiming tool transport actions elicited increased functional connectivity between the left SMG and bilateral posterior parietal cortices (see Figure 4c). A core function of the dorso-dorsal stream is to transform current visual input into a sensory-motor representation in the service of reaching and grasping, supported in part by bilateral IPS, superior parietal lobule, and dorsal premotor cortex. Although our analyses combined the planning and pantomiming phase when computing functional connectivity, in a supplemental analysis we measured functional connectivity modulated by the pantomiming phase of each trial, and found robust increases in functional connectivity driven by tool transport pantomiming between the left SMG and bilateral superior parietal lobule, bilateral dorsal premotor cortex, and bilateral somatosensory cortex (see Supporting Information Figure S3). Thus, generating a tool transport pantomime engages a bilateral network of regions consistent with the neuroanatomic substrates of the dorso-dorsal stream.

In a secondary aim, we measured functional connectivity between the left SMG and ventral temporal cortex (bilateral medial fusiform gyri and bilateral collateral sulci). Whereas previous work has reported functional connectivity between the left SMG and left medial fusiform gyrus during tool use tasks (e.g., see Garcea et al., 2018; Garcea &

Mahon, 2014), we found bilateral medial fusiform gyri exhibited differentially greater functional connectivity to the left SMG for tool transport planning and pantomiming, an action type emphasizing dorso-dorsal stream computations. To our knowledge this is the first study to contrast functional connectivity modulated by tool transport actions against tool use actions; thus it remains an open question whether the computations supported in part by medial ventral temporal cortex (e.g., processing of surface texture) are differentially relevant for tool transport actions relative to tool use actions. One prominent view proposed by Gallivan and Culham (2015) suggests that the ventral visual pathway may receive the outputs of visuomotor processes in frontal–parietal circuits prior to the onset of action (i.e., during the planning phase) to serve as a prediction mechanism of to-be performed actions. Consistent with this possibility, a recent lesion-activity mapping fMRI study in preoperative neurosurgery patients found that lesions involving the left SMG and adjacent voxels in the left anterior IPS were associated with reduced BOLD contrast for tools in the left medial fusiform gyrus, indicating that lesions to parietal action areas, including the left SMG, disrupt processing in the ventral visual pathway (Garcea et al., in press). Although speculative, in the tool transport condition the left SMG may query ventral stream representations of surface texture, as participants were instructed to imagine grasping the tool to move or transport it; in contrast, tool use epochs emphasize action kinematics and relative positioning of joint angles for accurate tool use, which may not emphasize to the same extent the processing of an object's material properties, including surface texture. It will also be important to consider if visual properties of tools facilitate tool use (e.g., that a keyboard has buttons that can be pressed) akin to structural affordances of tools that facilitate tool-directed grasping (e.g., that an object has a principal axis that "affords" grasping), and whether tool use affordances are neurocognitively distinct from structural and volumetric affordances of tools. Future functional connectivity research emphasizing diverse object properties when cueing an action (e.g., the coarseness of an object; that an object is slippery; that an object is heavy; e.g., see Cavina-Pratesi et al., 2018; Gallivan, Cant, Goodale, & Flanagan, 2014) can address the extent to which functional interactions between parietal action areas and ventral stream representations of objects are differentially modulated by the transport or use of manipulable objects.

A limitation of our study derives from the fact that tool transport gestures are more uniform and homogeneous than tool use gestures in terms of the structure of the hand and fingers for grasping, and in movement trajectory. While this limitation is not unique to our study (e.g., see Brandi et al., 2014), we designed our experiment such that participants explicitly planned and engaged in thinking about producing the action prior to physically generating a pantomime, permitting us to measure differences in BOLD contrast between tool use and tool transport actions independent of motoric differences between action types, and motoric similarity among tool transport actions. Furthermore, because every item was used in a tool use and tool transport epoch we know that the effects cannot reduce to low-level differences between the items, and instead must be driven by high-level processes that were differentially engaged by the task.

We also found that planning tool transport gestures engaged the right SMG to a greater extent than the left SMG (see Figure 3b). This may be due in part to the nature of the tool transport task (i.e., imagining picking an object up and passing it to a friend, or displacing it several inches), which may emphasize spatial imagery processes and encoding of the extrinsic position of the tool relative to the environment. Thus, it will be of interest for future research to consider how different tool-directed actions (e.g., pantomiming compared to imitation of use and transport actions) differentially engage right hemisphere regions.

5 | CONCLUSION

A number of fMRI studies have demonstrated there is a high degree of cross-talk between the dorsal and ventral visual pathways as a function of grasping or generating tool-directed gestures (e.g., see Budisavljevic, Dell'Acqua, & Castiello, 2018; Garcea et al., 2018; Hutchison & Gallivan, 2018) or when viewing objects or making judgments about object manipulation (e.g., Chen, Snow, Culham, & Goodale, 2018; Chen et al., 2017; Freud, Rosenthal, Ganel, & Avidan, 2015; Kleineberg et al., 2018; Sim, Helbig, Graf, & Kiefer, 2015; for discussion, see Orban & Caruana, 2014; van Polanen & Davare, 2015). Our results offer a novel interpretation of the role that the left SMG plays in tool-directed actions: Tool manipulation knowledge is not "represented" in the left SMG; rather the left SMG sits at the nexus of the dorso-dorsal and ventro-dorsal visual pathways, and serves as an intermediary or "hub" region aggregating (a) representations of object properties and conceptual knowledge in the ventral stream with (b) online sensory-motor information processed in the dorsal stream, (c) which is informed by top-down biasing signals from prefrontal cortex to resolve competition between candidate tool use actions. Future task-based functional connectivity studies using diverse tool-directed actions to bias processing to the ventro-dorsal or dorso-dorsal stream will permit a direct evaluation of these hypotheses and of the predictions of the 2AS+ model.

ACKNOWLEDGMENTS

The authors would like to thank Christine Watson and Harrison Stoll for their assistance in data collection. Preparation of this manuscript was supported by R01 NS099061 to L.J. Buxbaum, and by a Moss Rehabilitation Research Institute/University of Pennsylvania postdoctoral training fellowship (NIH 5T32HD071844-05).

ORCID

Frank E. Garcea https://orcid.org/0000-0002-8843-9127
Laurel J. Buxbaum https://orcid.org/0000-0003-2421-5455

REFERENCES

Andres, M., Pelgrims, B., & Olivier, E. (2013). Distinct contribution of the parietal and temporal cortex to hand configuration and contextual judgements about tools. *Cortex*, *49*(8), 2097–2105. https://doi.org/10.1016/j.cortex.2012.11.013

Anzellotti, S., Mahon, B. Z., Schwarzbach, J., & Caramazza, A. (2011). Differential activity for animals and manipulable objects in the anterior temporal lobes. *Journal of Cognitive Neuroscience*, *23*(8), 2059–2067. https://doi.org/10.1162/jocn.2010.21567

Beauchamp, M. S., Lee, K. E., Haxby, J. V., & Martin, A. (2002). Parallel visual motion processing streams for manipulable objects and human movements. *Neuron*, *34*(1), 149–159.

Binkofski, F., & Buxbaum, L. J. (2013). Two action systems in the human brain. *Brain and Language*, *127*(2), 222–229. https://doi.org/10.1016/j.bandl.2012.07.007

Boronat, C. B., Buxbaum, L. J., Coslett, H. B., Tang, K., Saffran, E. M., Kimberg, D. Y., & Detre, J. A. (2005). Distinctions between manipulation and function knowledge of objects: Evidence from functional magnetic resonance imaging. *Brain Research. Cognitive Brain Research*, *23*(2–3), 361–373. https://doi.org/10.1016/j.cogbrainres.2004.11.001

Brambati, S. M., Myers, D., Wilson, A., Rankin, K. P., Allison, S. C., Rosen, H. J., … Gorno-Tempini, M. L. (2006). The anatomy of category-specific object naming in neurodegenerative diseases. *Journal of Cognitive Neuroscience*, *18*(10), 1644–1653. https://doi.org/10.1162/jocn.2006.18.10.1644

Brandi, M. L., Wohlschlager, A., Sorg, C., & Hermsdorfer, J. (2014). The neural correlates of planning and executing actual tool use. *The Journal of Neuroscience*, *34*(39), 13183–13194. https://doi.org/10.1523/JNEUROSCI.0597-14.2014

Buchwald, M., Przybylski, L., & Kroliczak, G. (2018). Decoding brain states for planning functional grasps of tools: A functional magnetic resonance imaging multivoxel pattern analysis study. *Journal of the International Neuropsychological Society*, *24*(10), 1013–1025. https://doi.org/10.1017/S1355617718000590

Budisavljevic, S., Dell'Acqua, F., & Castiello, U. (2018). Cross-talk connections underlying dorsal and ventral stream integration during hand actions. *Cortex*, *103*, 224–239. https://doi.org/10.1016/j.cortex.2018.02.016

Buxbaum, L. J. (2017). Learning, remembering, and predicting how to use tools: Distributed neurocognitive mechanisms: Comment on Osiurak and Badets (2016). *Psychological Review*, *124*(3), 346–360. https://doi.org/10.1037/rev0000051

Buxbaum, L. J., Kyle, K. M., Tang, K., & Detre, J. A. (2006). Neural substrates of knowledge of hand postures for object grasping and functional object use: Evidence from fMRI. *Brain Research*, *1117*(1), 175–185. https://doi.org/10.1016/j.brainres.2006.08.010

Campanella, F., D'Agostini, S., Skrap, M., & Shallice, T. (2010). Naming manipulable objects: Anatomy of a category specific effect in left temporal tumours. *Neuropsychologia*, *48*(6), 1583–1597. https://doi.org/10.1016/j.neuropsychologia.2010.02.002

Canessa, N., Borgo, F., Cappa, S. F., Perani, D., Falini, A., Buccino, G., … Shallice, T. (2008). The different neural correlates of action and functional knowledge in semantic memory: An FMRI study. *Cerebral Cortex*, *18*(4), 740–751. https://doi.org/10.1093/cercor/bhm110

Cant, J. S., & Goodale, M. A. (2007). Attention to form or surface properties modulates different regions of human occipitotemporal cortex. *Cerebral Cortex*, *17*(3), 713–731. https://doi.org/10.1093/cercor/bhk022

Cavina-Pratesi, C., Connolly, J. D., Monaco, S., Figley, T. D., Milner, A. D., Schenk, T., & Culham, J. C. (2018). Human neuroimaging reveals the subcomponents of grasping, reaching and pointing actions. *Cortex*, *98*, 128–148. https://doi.org/10.1016/j.cortex.2017.05.018

Chao, L. L., Haxby, J. V., & Martin, A. (1999). Attribute-based neural substrates in temporal cortex for perceiving and knowing about objects. *Nature Neuroscience*, *2*(10), 913–919. https://doi.org/10.1038/13217

Chao, L. L., & Martin, A. (2000). Representation of manipulable man-made objects in the dorsal stream. *NeuroImage*, *12*(4), 478–484. https://doi.org/10.1006/nimg.2000.0635

Chen, J., Snow, J. C., Culham, J. C., & Goodale, M. A. (2018). What role does "elongation" play in "tool-specific" activation and connectivity in the dorsal and ventral visual streams? *Cerebral Cortex*, *28*(4), 1117–1131. https://doi.org/10.1093/cercor/bhx017

Chen, Q., Garcea, F. E., Almeida, J., & Mahon, B. Z. (2017). Connectivity-based constraints on category-specificity in the ventral object processing pathway. *Neuropsychologia*, *105*, 184–196. https://doi.org/10.1016/j.neuropsychologia.2016.11.014

Chen, Q., Garcea, F. E., Jacobs, R. A., & Mahon, B. Z. (2018). Abstract representations of object-directed action in the left inferior parietal lobule. *Cerebral Cortex*, *26*, 2162–2174. https://doi.org/10.1093/cercor/bhx120

Chen, Q., Garcea, F. E., & Mahon, B. Z. (2016). The representation of object-directed action and function knowledge in the human brain. *Cerebral Cortex*, *26*(4), 1609–1618. https://doi.org/10.1093/cercor/bhu328

Cisek, P., & Kalaska, J. F. (2010). Neural mechanisms for interacting with a world full of action choices. *Annual Review of Neuroscience*, *33*, 269–298. https://doi.org/10.1146/annurev.neuro.051508.135409

Cloutman, L. L. (2013). Interaction between dorsal and ventral processing streams: Where, when and how? *Brain and Language*, *127*(2), 251–263. https://doi.org/10.1016/j.bandl.2012.08.003

Devlin, J. T., Rushworth, M. F., & Matthews, P. M. (2005). Category-related activation for written words in the posterior fusiform is task specific. *Neuropsychologia*, *43*(1), 69–74. https://doi.org/10.1016/j.neuropsychologia.2004.06.013

Erdogan, G., Chen, Q., Garcea, F. E., Mahon, B. Z., & Jacobs, R. A. (2016). Multisensory part-based representations of objects in human lateral occipital cortex. *Journal of Cognitive Neuroscience*, *28*(6), 869–881. https://doi.org/10.1162/jocn_a_00937

Freud, E., Plaut, D. C., & Behrmann, M. (2016). 'What' is happening in the dorsal visual pathway. *Trends in Cognitive Sciences*, *20*(10), 773–784. https://doi.org/10.1016/j.tics.2016.08.003

Freud, E., Rosenthal, G., Ganel, T., & Avidan, G. (2015). Sensitivity to object impossibility in the human visual cortex: Evidence from functional connectivity. *Journal of Cognitive Neuroscience*, *27*(5), 1029–1043. https://doi.org/10.1162/jocn_a_00753

Gallivan, J. P., Cant, J. S., Goodale, M. A., & Flanagan, J. R. (2014). Representation of object weight in human ventral visual cortex. *Current Biology*, *24*(16), 1866–1873. https://doi.org/10.1016/j.cub.2014.06.046

Gallivan, J. P., & Culham, J. C. (2015). Neural coding within human brain areas involved in actions. *Current Opinion in Neurobiology*, *33*, 141–149. https://doi.org/10.1016/j.conb.2015.03.012

Gallivan, J. P., McLean, D. A., Valyear, K. F., & Culham, J. C. (2013). Decoding the neural mechanisms of human tool use. *eLife*, *2*, e00425. https://doi.org/10.7554/eLife.00425

Garcea, F. E., Almeida, J., Sims, M. H., Nunno, A., Meyers, S. P., Li, Y. M., … Mahon, B. Z. (in press, 2020). Domain-specific Diaschisis: Lesions to parietal action areas modulate neural responses to tools in the ventral stream. *Cereb Cortex*. https://doi.org/10.1093/cercor/bhy183

Garcea, F. E., Chen, Q., Vargas, R., Narayan, D. A., & Mahon, B. Z. (2018). Task- and domain-specific modulation of functional connectivity in the ventral and dorsal object-processing pathways. *Brain Structure & Function*, *223*, 2589–2607. https://doi.org/10.1007/s00429-018-1641-1

Garcea, F. E., Kristensen, S., Almeida, J., & Mahon, B. Z. (2016). Resilience to the contralateral visual field bias as a window into object representations. *Cortex*, *81*, 14–23. https://doi.org/10.1016/j.cortex.2016.04.006

Garcea, F. E., & Mahon, B. Z. (2014). Parcellation of left parietal tool representations by functional connectivity. *Neuropsychologia*, *60*, 131–143. https://doi.org/10.1016/j.neuropsychologia.2014.05.018

Garcea, F. E., & Mahon, B. Z. (in press). The how and what of object knowledge in the human brain. In N. O. Schiller & G. de Zubicaray (Eds.). *The Oxford handbook of Neurolinguistics* (pp. 576–602) Oxford, UK: Oxford University Press.

Goldenberg, G., Hermsdorfer, J., Glindemann, R., Rorden, C., & Karnath, H. O. (2007). Pantomime of tool use depends on integrity of left inferior frontal cortex. *Cerebral Cortex*, *17*(12), 2769–2776. https://doi.org/10.1093/cercor/bhm004

Gonzalez-Castillo, J., & Bandettini, P. A. (2017). Task-based dynamic functional connectivity: Recent findings and open questions. *NeuroImage*, *180*, 526–533. https://doi.org/10.1016/j.neuroimage.2017.08.006

Gotts, S. J., Jo, H. J., Wallace, G. L., Saad, Z. S., Cox, R. W., & Martin, A. (2013). Two distinct forms of functional lateralization in the human brain. *Proceedings of the National Academy of Sciences of the United States of America*, *110*(36), E3435–E3444. https://doi.org/10.1073/pnas.1302581110

Gotts, S. J., Saad, Z. S., Jo, H. J., Wallace, G. L., Cox, R. W., & Martin, A. (2013). The perils of global signal regression for group comparisons: A case study of autism Spectrum disorders. *Frontiers in Human Neuroscience*, *7*, 356. https://doi.org/10.3389/fnhum.2013.00356

Grafton, S. T., Fadiga, L., Arbib, M. A., & Rizzolatti, G. (1997). Premotor cortex activation during observation and naming of familiar tools. *NeuroImage*, *6*(4), 231–236. https://doi.org/10.1006/nimg.1997.0293

Hamzei, F., Vry, M. S., Saur, D., Glauche, V., Hoeren, M., Mader, I., … Rijntjes, M. (2016). The dual-loop model and the human Mirror neuron system: An exploratory combined fMRI and DTI study of the inferior

frontal Gyrus. *Cerebral Cortex*, *26*(5), 2215–2224. https://doi.org/10.1093/cercor/bhv066

Hermsdorfer, J., Terlinden, G., Muhlau, M., Goldenberg, G., & Wohlschlager, A. M. (2007). Neural representations of pantomimed and actual tool use: Evidence from an event-related fMRI study. *NeuroImage*, *36*(Suppl 2), T109–T118. https://doi.org/10.1016/j.neuroimage.2007.03.037

Hutchison, R. M., & Gallivan, J. P. (2018). Functional coupling between frontoparietal and occipitotemporal pathways during action and perception. *Cortex*, *98*, 8–27. https://doi.org/10.1016/j.cortex.2016.10.020

Ishibashi, R., Lambon Ralph, M. A., Saito, S., & Pobric, G. (2011). Different roles of lateral anterior temporal lobe and inferior parietal lobule in coding function and manipulation tool knowledge: Evidence from an rTMS study. *Neuropsychologia*, *49*(5), 1128–1135. https://doi.org/10.1016/j.neuropsychologia.2011.01.004

Johnson-Frey, S. H., Maloof, F. R., Newman-Norlund, R., Farrer, C., Inati, S., & Grafton, S. T. (2003). Actions or hand-object interactions? Human inferior frontal cortex and action observation. *Neuron*, *39*(6), 1053–1058.

Johnson-Frey, S. H., Newman-Norlund, R., & Grafton, S. T. (2005). A distributed left hemisphere network active during planning of everyday tool use skills. *Cerebral Cortex*, *15*(6), 681–695. https://doi.org/10.1093/cercor/bhh169

Kalenine, S., & Buxbaum, L. J. (2016). Thematic knowledge, artifact concepts, and the left posterior temporal lobe: Where action and object semantics converge. *Cortex*, *82*, 164–178. https://doi.org/10.1016/j.cortex.2016.06.008

Kellenbach, M. L., Brett, M., & Patterson, K. (2003). Actions speak louder than functions: The importance of manipulability and action in tool representation. *Journal of Cognitive Neuroscience*, *15*(1), 30–46. https://doi.org/10.1162/089892903321107800

Kleineberg, N. N., Dovern, A., Binder, E., Grefkes, C., Eickhoff, S. B., Fink, G. R., & Weiss, P. H. (2018). Action and semantic tool knowledge—Effective connectivity in the underlying neural networks. *Human Brain Mapping*, *39*, 3473–3486. https://doi.org/10.1002/hbm.24188

Konen, C. S., Mruczek, R. E., Montoya, J. L., & Kastner, S. (2013). Functional organization of human posterior parietal cortex: Grasping- and reaching-related activations relative to topographically organized cortex. *Journal of Neurophysiology*, *109*(12), 2897–2908. https://doi.org/10.1152/jn.00657.2012

Kriegeskorte, N., Simmons, W. K., Bellgowan, P. S., & Baker, C. I. (2009). Circular analysis in systems neuroscience: The dangers of double dipping. *Nature Neuroscience*, *12*(5), 535–540. https://doi.org/10.1038/nn.2303

Kristensen, S., Garcea, F. E., Mahon, B. Z., & Almeida, J. (2016). Temporal frequency tuning reveals interactions between the dorsal and ventral visual streams. *Journal of Cognitive Neuroscience*, *28*(9), 1295–1302. https://doi.org/10.1162/jocn_a_00969

Kroliczak, G., & Frey, S. H. (2009). A common network in the left cerebral hemisphere represents planning of tool use pantomimes and familiar intransitive gestures at the hand-independent level. *Cerebral Cortex*, *19*(10), 2396–2410. https://doi.org/10.1093/cercor/bhn261

Kundu, P., Brenowitz, N. D., Voon, V., Worbe, Y., Vertes, P. E., Inati, S. J., … Bullmore, E. T. (2013). Integrated strategy for improving functional connectivity mapping using multiecho fMRI. *Proceedings of the National Academy of Sciences of the United States of America*, *110*(40), 16187–16192. https://doi.org/10.1073/pnas.1301725110

Kundu, P., Inati, S. J., Evans, J. W., Luh, W. M., & Bandettini, P. A. (2012). Differentiating BOLD and non-BOLD signals in fMRI time series using multi-echo EPI. *NeuroImage*, *60*(3), 1759–1770. https://doi.org/10.1016/j.neuroimage.2011.12.028

Lewis, J. W. (2006). Cortical networks related to human use of tools. *The Neuroscientist*, *12*(3), 211–231. https://doi.org/10.1177/1073858406288327

Lingnau, A., & Downing, P. E. (2015). The lateral occipitotemporal cortex in action. *Trends in Cognitive Sciences*, *19*(5), 268–277. https://doi.org/10.1016/j.tics.2015.03.006

Mahon, B. Z., Anzellotti, S., Schwarzbach, J., Zampini, M., & Caramazza, A. (2009). Category-specific organization in the human brain does not require visual experience. *Neuron*, *63*(3), 397–405. https://doi.org/10.1016/j.neuron.2009.07.012

Mahon, B. Z., & Caramazza, A. (2011). What drives the organization of object knowledge in the brain? *Trends in Cognitive Sciences*, *15*(3), 97–103. https://doi.org/10.1016/j.tics.2011.01.004

Mahon, B. Z., Milleville, S. C., Negri, G. A., Rumiati, R. I., Caramazza, A., & Martin, A. (2007). Action-related properties shape object representations in the ventral stream. *Neuron*, *55*(3), 507–520. https://doi.org/10.1016/j.neuron.2007.07.011

Martin, A. (2007). The representation of object concepts in the brain. *Annual Review of Psychology*, *58*, 25–45. https://doi.org/10.1146/annurev.psych.57.102904.190143

Martin, M., Beume, L., Kummerer, D., Schmidt, C. S., Bormann, T., Dressing, A., … Weiller, C. (2016). Differential roles of ventral and dorsal streams for conceptual and production-related components of tool use in acute stroke patients. *Cerebral Cortex*, *26*(9), 3754–3771. https://doi.org/10.1093/cercor/bhv179

Milner, A. D. (2017). How do the two visual streams interact with each other? *Experimental Brain Research*, *235*(5), 1297–1308. https://doi.org/10.1007/s00221-017-4917-4

Noppeney, U., Price, C. J., Penny, W. D., & Friston, K. J. (2006). Two distinct neural mechanisms for category-selective responses. *Cerebral Cortex*, *16*(3), 437–445. https://doi.org/10.1093/cercor/bhi123

Oldfield, R. C. (1971). The assessment and analysis of handedness: The Edinburgh inventory. *Neuropsychologia*, *9*(1), 97–113.

Orban, G. A., & Caruana, F. (2014). The neural basis of human tool use. *Frontiers in Psychology*, *5*, 310. https://doi.org/10.3389/fpsyg.2014.00310

Pelgrims, B., Olivier, E., & Andres, M. (2011). Dissociation between manipulation and conceptual knowledge of object use in the supramarginalis gyrus. *Human Brain Mapping*, *32*(11), 1802–1810. https://doi.org/10.1002/hbm.21149

Pobric, G., Jefferies, E., & Ralph, M. A. (2010). Amodal semantic representations depend on both anterior temporal lobes: Evidence from repetitive transcranial magnetic stimulation. *Neuropsychologia*, *48*(5), 1336–1342. https://doi.org/10.1016/j.neuropsychologia.2009.12.036

Rizzolatti, G., & Matelli, M. (2003). Two different streams form the dorsal visual system: Anatomy and functions. *Experimental Brain Research*, *153*(2), 146–157. https://doi.org/10.1007/s00221-003-1588-0

Rumiati, R. I., Weiss, P. H., Shallice, T., Ottoboni, G., Noth, J., Zilles, K., & Fink, G. R. (2004). Neural basis of pantomiming the use of visually presented objects. *NeuroImage*, *21*(4), 1224–1231. https://doi.org/10.1016/j.neuroimage.2003.11.017

Saad, Z. S., Reynolds, R. C., Jo, H. J., Gotts, S. J., Chen, G., Martin, A., & Cox, R. W. (2013). Correcting brain-wide correlation differences in resting-state FMRI. *Brain Connectivity*, *3*(4), 339–352. https://doi.org/10.1089/brain.2013.0156

Schubotz, R. I., Wurm, M. F., Wittmann, M. K., & von Cramon, D. Y. (2014). Objects tell us what action we can expect: Dissociating brain areas for retrieval and exploitation of action knowledge during action observation in fMRI. *Frontiers in Psychology*, *5*, 636. https://doi.org/10.3389/fpsyg.2014.00636

Sim, E. J., Helbig, H. B., Graf, M., & Kiefer, M. (2015). When action observation facilitates visual perception: Activation in visuo-motor areas contributes to object recognition. *Cerebral Cortex*, *25*(9), 2907–2918. https://doi.org/10.1093/cercor/bhu087

Simmons, W. K., & Martin, A. (2012). Spontaneous resting-state BOLD fluctuations reveal persistent domain-specific neural networks. *Social Cognitive and Affective Neuroscience*, *7*(4), 467–475. https://doi.org/10.1093/scan/nsr018

Talairach, J., & Tournoux, P. (1988). *Co-planar stereotaxic atlas of the human brain 3-dimensional proportional system: An approach to cerebral imaging*. New York: Thieme Medical Publishers.

Valyear, K. F., & Culham, J. C. (2010). Observing learned object-specific functional grasps preferentially activates the ventral stream. *Journal of Cognitive Neuroscience*, *22*(5), 970–984. https://doi.org/10.1162/jocn.2009.21256

van Polanen, V., & Davare, M. (2015). Interactions between dorsal and ventral streams for controlling skilled grasp. *Neuropsychologia*, *79*(Pt B), 186–191. https://doi.org/10.1016/j.neuropsychologia.2015.07.010

Vry, M. S., Tritschler, L. C., Hamzei, F., Rijntjes, M., Kaller, C. P., Hoeren, M., … Weiller, C. (2015). The ventral fiber pathway for pantomime of object use. *NeuroImage*, *106*, 252–263. https://doi.org/10.1016/j.neuroimage.2014.11.002

Watson, C. E., & Buxbaum, L. J. (2015). A distributed network critical for selecting among tool-directed actions. *Cortex*, *65*, 65–82. https://doi.org/10.1016/j.cortex.2015.01.007

SUPPORTING INFORMATION

Additional supporting information may be found online in the Supporting Information section at the end of this article.

How to cite this article: Garcea FE, Buxbaum LJ. Gesturing tool use and tool transport actions modulates inferior parietal functional connectivity with the dorsal and ventral object processing pathways. *Hum Brain Mapp*. 2019;40:2867–2883. https://doi.org/10.1002/hbm.24565